Journal of Power Sources 183 (2008) 431–435

Contents lists available at ScienceDirect

Journal of Power Sources

journal homepage: www.elsevier.com/locate/jpowsour

Short communication

Effect of P_2O_5 in Li_2O–P_2O_5–B_2O_3 electrolyte fabricated by aerosol flame deposition☆

Kihyun Cho, Jangwon Oh, Taewon Lee, Dongwook Shin*

Division of Material Science & Engineering, Hanyang University, 17 Haengdang-dong, Seongdong-gu, Seoul 133-791, Republic of Korea

ARTICLE INFO

Article history:
Available online 18 May 2008

Keywords:
Li_2O–B_2O_3–P_2O_5
Aerosol flame deposition
Thin film battery
Solid electrolyte
Glass electrolyte

ABSTRACT

Amorphous Li_2O–B_2O_3–P_2O_5 films were fabricated using "aerosol flame deposition (AFD)" method for the thin film battery application. The liquid or gas type precursor sources such as Li precursor solutions, BCl_3 and $POCl_3$ were used to fabricate the electrolyte films. In this work, we studied the effect of P_2O_5 in a LiO_2–P_2O_5–B_2O_3 system formed at various flow rates of $POCl_3$. XRD analysis revealed that the crystalline phase of H_3BO_3 as well as other oxides was formed in glass soot. As the flow rate of $POCl_3$ increased, the glass soot gradually changed to amorphous phase. The ionic conductivity of the soot was measured and the FT-IR and Raman spectroscopy were used to correlate the measured conductivity to the glass network structure in the deposited soot film. The maximum conductivity of electrolyte prepared at conditions of 20 sccm flow rate of BCl_3 and 80 sccm flow rate of $POCl_3$ was 2×10^{-6} at room temperature. As P_2O_5 contents increased, the conductivity of glass electrolyte increased due to the increase of P—O structural unit associated with non-bridging oxygens (NBO).

1. Introduction

Rechargeable thin film battery with small, light-weight, and reasonable capacity have been studied for small electronic devices, such as active RF card, micro robot and meso-machines (MEMS). However, solid-state lithium batteries have not been commercialized for practical applications due to various limitations. Among the limitation, the solid electrolyte and the interfacial problems related to this electrolyte are major obstacles to be overcome. For practical application, solid electrolyte of the thin film battery must have high ionic conductivity and chemical, thermal and electrochemical stability. Glass electrolytes may be divided into chalcogenides and oxide glasses. Although chalcogenides glasses have a good conductivity, these have several drawbacks such as corrosive chemical nature of sulfur resulting in the difficulty in handling and managing the fabrication, highly hygroscopic nature, the stability in air, the inertness to the reaction with electrodes, and so on. Due to these problems chalcogenides glass electrolytes have not yet been developed for real application. Recently, many researchers have tried to develop materials with these properties and fabrication processes for solid electrolytes of various types by using oxide glasses. Researchers have attempted to understand the conductivity and structure of Li_2O–P_2O_5 and Li_2O–B_2O_3 glasses by using melting and quenching method. Boron and phosphorus oxide are well-known as the glass formers. Lithium oxide is a glass network modifier, which offers a mobile charge carrier, Li^+.

The structure of pure vitreous B_2O_3 consists of a random network of boroxol rings and BO_3 triangles connected by a B—O—B linkages (bridging oxygen atom) [1]. The addition of alkali oxides modifies the boroxol ring; complex borate groups with one or two 4-coordinated boron atoms are formed [2].

Angell and co-workers [3,4] had studied the Li_2O–P_2O_5 glass system. The conductivity at room temperature varies from 10^{-6} to 10^{-11} as Li_2O content. Structural analysis showed that the addition of Li_2O breaks up P═O bridges, creating non-bridging oxygens (NBO). However, unlike phosphate and borate glasses, there are not many researches on boronphosphate glasses. In spite of their high ionic conductivity, the phosphate or borate glasses are not suitable for the practical application due to their highly hygroscopic nature and subsequent devitrification. On the other hand, borophosphate glass is relatively stable to devitrification compared to borate or phosphate glasses.

Preliminary work in our laboratory using bulk type glasses showed that the ratio of P_2O_5 to B_2O_3 has profound effect on the Li ion conductivity [5]. In this work, we have developed the deposition method, which is called the "aerosol flame deposition (AFD)," for the fabrication of the Li_2O–B_2O_3–P_2O_5 glass electrolyte film. In this process, $LiNO_3$, $POCl_3$ and BCl_3 were hydrolyzed in an oxy-hydrogen flame and converted into oxide by hydrolysis reaction and grown to particles by the nucleation and subsequent Brownian

☆ Selected papers presented at the IMLB 2006—International Meeting on Lithium Batteries.

* Corresponding author. Tel.: +82 2 2220 0503; fax: +82 2 2299 3851.
E-mail address: dwshin@hanyang.ac.kr (D. Shin).

0378-7753/$ – see front matter © 2008 Elsevier B.V. All rights reserved.
doi:10.1016/j.jpowsour.2008.05.029

coagulation. The effect of P_2O_5 in Li_2O–B_2O_3–P_2O_5 glass electrolyte formed by aerosol flame deposition was studied using the FT-IR, X-ray diffraction and Raman spectroscopy. The correlation between the conductivity and structural characteristics of the glass electrolyte was analyzed.

2. Experiments

The precursor solution of lithium was prepared by dissolving lithium nitrate in methanol at a concentration of 0.5 mol%. The droplet of lithium precursor generated by nebulizer with the ultrasonic resonator (1.7 MHz) was carried into the flame made at conditions of the oxygen flow rate of 7.5 L min^{-1}, Ar shield flow rate of 3 L min^{-1}, and hydrogen flow rate of 1.5 L min^{-1}.

The vapors of bubbled $POCl_3$ and BCl_3 under controlled temperature were delivered to an oxy-hydrogen torch and hydrolyzed in the flame to form porous oxide soot film on Si substrates. To observe the effect of $POCl_3$ the flow rate of BCl_3 was fixed at 20 sccm while the flow rates of $POCl_3$ were increased 30, 60, and 80 sccm.

To remove the surface sintering caused by the flame and to deposit thin film of uniform thickness, oxide soot particles were deposited on a silicon or quartz glass substrate placed in a programmed rotating stage, which was kept at 150 °C to eliminate H_2O produced during the fuel reaction of hydrogen and oxygen. The porous oxide soot was sintered into dense film in a furnace at 600 °C for 2 h.

To carry out the various measurements, the specimen was prepared from the soot collected from the deposited films by melting them in a Pt crucible at 1000 °C. X-ray diffraction analysis was performed to confirm the effect of phosphorus oxide and to check the crystalline phases of deposited films after heat treatment.

To measure the ionic conductivities the amorphous glass electrolytes were painted by silver paste on both sides of the glass electrolyte as ion blocking electrodes. Conductivity was measured by a complex impedance method using Solartron 1260 impedance analyzer with an ac voltage of 50 mV amplitude over the frequency range 100 mHz–10 MHz at room temperatures.

For the comparison with thin film electrolyte, bulk glasses with composition $45Li_2O$–$55((1-x)B_2O_3$–$xP_2O_5)$ were prepared by using a melting and quenching method from reagents grade material (99% Li_2CO_3, 98% P_2O_5 and 95% B_2O_3).

The correlation between the structural modification of glass network and the composition of the electrolyte produced by heat treatment was characterized by FT-IR and Raman spectroscopy as a function of the chemical composition. Glass electrolyte were ground and mixed with KBr in a 1:100 weight ratio and pressed into pellets to obtain the infrared spectra (FTLA 2000-100) in the range from 500 to 4000 cm^{-1}. The Raman spectra of the glasses were measured using laser Raman Spectrophotometer (JASCO NRS-3100) with 514 nm argon laser in 200–1400 cm^{-1} range under air atmosphere.

The notations for the prepared specimen are the abbreviation of the flow rate of these source gases for glass formers. For example, B20P30 denotes the specimen prepared at the flow rate of 20 sccm of BCl_3 and 30 sccm of $POCl_3$.

3. Results and discussion

The source gases of BCl_3 and $POCl_3$ has been proved to transform into oxide particles by using the flame and hydrolysis reaction [6]. In this reaction, the formed oxides particles were mixtures of amorphous oxides and hydrate, whose proportion is determined by the flow rates of BCl_3 and $POCl_3$ as shown in Fig. 1. The crystalline H_3BO_3 was formed under the flow rates of 20 sccm of BCl_3 and

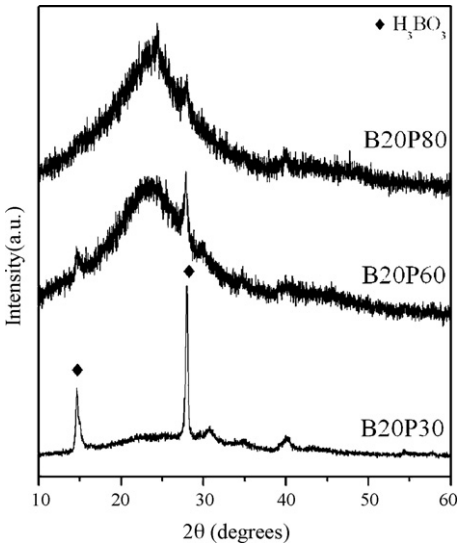

Fig. 1. X-ray diffraction patterns of soot film produced at various flow rates of $POCl_3$ by aerosol flame deposition.

30 sccm of $POCl_3$. As the flow rate of $POCl_3$ was increased, this peak was changed to a broad diffraction peak centered at $2\theta = 21°$ while intensity of the crystalline H_3BO_3 was decreased. The reduction of the crystalline H_3BO_3 might be due to the reduced proportion of hygroscopic boron within the synthesized soot.

The formed crystalline H_3BO_3 was not considered serious since it converted into B_2O_3 by brief heat treatment.

Li source, an aqueous $LiNO_3$, supplied from the aerosol system has no effect on the XRD pattern, which suggests that amorphous Li_2O was formed or Li ion incorporated into glass particles as ions. There was no sign of the formation of Li_2CO_3 although this phase is known to be formed in the similar reaction environment [7]. The deposited Li_2O–P_2O_5–B_2O_3 glass soot was investigated by FT-IR spectra as a function of $POCl_3$ which is summarized in Fig. 2. From the literature [8], the crystalline H_3BO_3 have sharp absorbance around 1200, 880, 650, and 550 cm^{-1}. The broad bands in the range

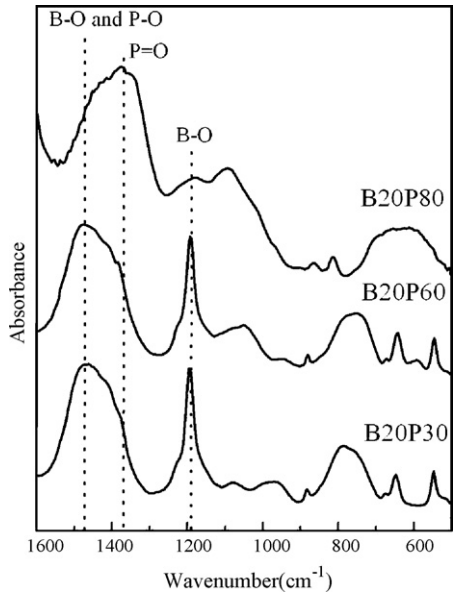

Fig. 2. FT-IR spectra of glass soot film produced at various flow rates of $POCl_3$ by aerosol flame deposition.

of 1300–1550 cm^{-1} can be attributed to borate units and the phosphoryl group [9–11]. As the flow rate of $POCl_3$ was increased, in the FT-IR spectrum of glass soot produced by aerosol flame deposition, the peak at 1470 cm^{-1}, the band of B—O group, reduced significantly due to the increased proportion of P═O bond. The sharp peak at 1200 cm^{-1} almost disappeared in B20P80 specimen, which supports the observation in XRD patterns. In this specimen, the broad bands in the range of 550–700 cm^{-1} also grew by the symmetric P—O—P groups [12].

After heat treatment at 1000 °C, as shown in Fig. 3, X-ray diffraction patterns of glass soot films show complete amorphous patterns except B20P30. The B_2O_3 converted from H_3BO_3 was observed in B20P30 glass specimens as a minor phase, which is a phase normally observed in the cancined glass with high concentration of H_3BO_3. However, the glass soot with low concentration of H_3BO_3 completely disappeared by heat treatment. It is worth to notice that the peak at $2\theta = 28°$ is assigned to B_2O_3 rather than H_3BO_3 since the peak at $2\theta = 15°$ is absent in the calcined specimen and FT-IR peak at 1200 cm^{-1} was confirmed to disappear as shown in Fig. 2.

The lithium ion conductivity is determined mainly by the concentration of lithium ion in glass network and the structural modification of glass formers induced by this ion [13–16]. The combination of these two effects increases the ionic conduction of glass electrolyte. However, the modification of network structure can be induced by changing the composition of glass formers and this alters the 'free volume' of glass network. The free volume within glass network is expected to free up more immobile Li ions trapped in the deep energy level and converts these immobile ions into mobile charge carrier. Therefore, although less evident than the case of the addition of Li ion, the conductivity increases as the result of increase in the number of effective mobile ions and the reduction of the activation energy of mobility. Non-bridging oxygen generated by alkali oxides is known to offer the hoping site for ionic conduction in oxide glass network [17]. The formation of non-bridging oxygen is also contributing to the formation of relatively open network structure with large free volume for ion drift.

Fig. 4(a) shows typical Nyquist plots of the Li_2O–B_2O_3–P_2O_5 glass system formed at various flow rates of $POCl_3$ at room temperature. Nyquist plots of the specimen B20P30 appeared tailed in low frequency range due to the crystalline B_2O_3. The conductivity of the thin film electrolyte determined from the Nyquist plot is shown in Fig. 4(b) and compared to that of bulk glass electrolyte as a function of the ratios of network former, P/(B + P). The conductivity of bulk electrolyte prepared by melting and quenching method was the highest at P/(B + P) = 0.5, which is the result of the maximized number of non-bridging oxygen site and even distribution of Li ion throughout the P—O, B—O, and B—O—P bonds. The increase of conductivity under P/(B + P) = 0.5 is due to the increase of non-bridging oxygen, while the decrease over P/(B + P) = 0.5 is due to the preferential segregation of Li ion to P—O chains caused by the partial devitrification of B—O chains[18].

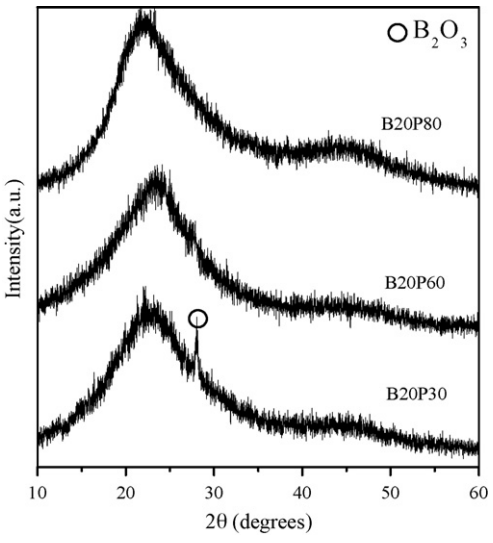

Fig. 3. XRD patterns of glass electrolyte fabricated from the deposited glass soot.

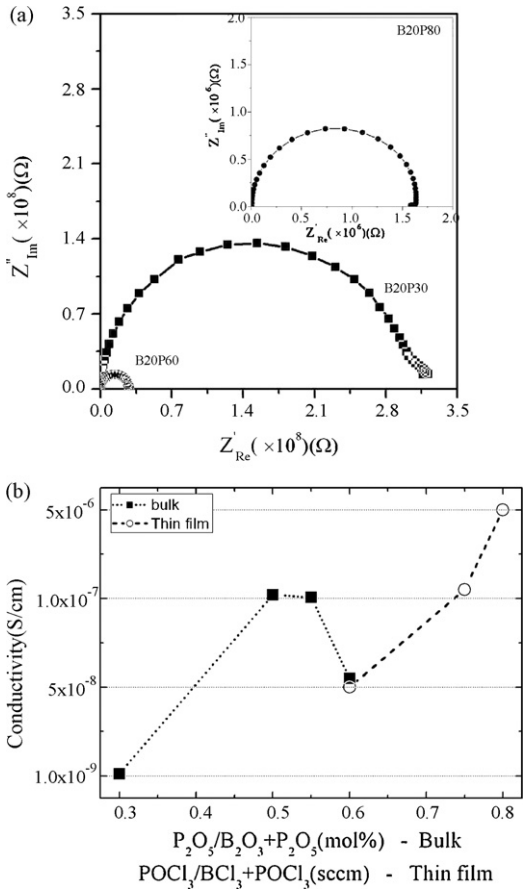

Fig. 4. (a) Nyquist plots of glass electrolyte at various flow rate of $POCl_3$ and (b) the measured conductivity of the thin film electrolyte (○) and the bulk electrolyte (■) prepared by melting and quenching.

In the thin film electrolyte fabricated by aerosol flame deposition, the conductivity did not exhibit the similar trend to that in the bulk glass. As the P/(B + P) increased, the lithium ion conductivity of glass electrolyte kept increasing. Maximum ionic conductivity of the electrolyte film was about 10^{-6} S cm^{-1} at room temperature, which is higher than that of bulk electrolyte glass.

The difference between the bulk glass and thin film glass is very interesting and invokes several speculations on the possible reasons. First of all, the process for the bulk glass requires higher temperature and longer time for the homogeneous melting and, hence, this increases the probability of devitrification. Practical experience supports this tendency, so that the glass with P/(B + P) > 0.5 is hard to obtain in melting and quenching process. In contrary, thin film type glass composed of nano sized soot particle can be sintered at relatively lower temperature and time. Therefore, the higher concentration of P_2O_5 enabled the higher maximum conductivity. Another possible reason is that the quenching rate the glass experienced is higher for the thin film type glass electrolyte. Aerosol flame deposition process produces the glass soot particle

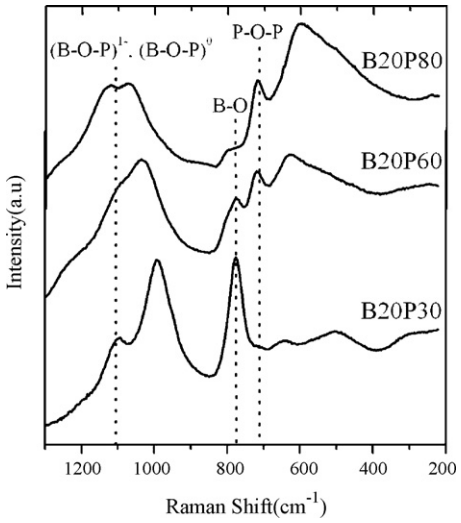

Fig. 5. Raman spectra of glass electrolyte fabricated from the deposited glass soot.

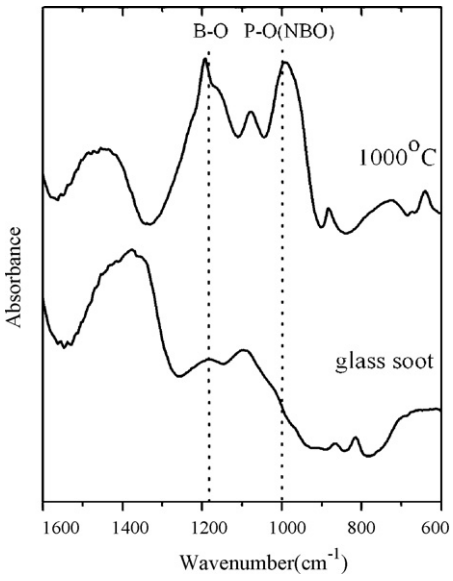

Fig. 6. FT-IR spectra compared to soot and electrolyte of B20P80.

within an oxy-hydrogen flame whose temperature is 1300–1800 °C. Therefore, the glass soot particles experience much higher quenching rate than the bulk glass does. In glass, the higher quenching rate generally produces the more open network structure, which results in the higher mobility and/or larger number of the effective charge carrier.

Relationship between the variation of non-bridging oxygen content and conductivity was investigated by Raman and FT-IR spectra. The Raman spectra observed in the specimen B20P30 was similar to that of borate glass with lithium ion, as shown in Fig. 5. This is due to low synthesis rate of P_2O_5 compared to B_2O_3 even under the same flow rate of both source gases and intense evaporation of P_2O_5 due to its volatile nature. The Raman peak observed at 806 cm^{-1} is assigned to the vibration of pure B_2O_3 with B—O bonding in boroxol ring without non-bridging oxygen and reported to shift to lower wavenumber and broadened with increasing Li concentration [19–21]. The peak around 780 cm^{-1} shifted from pure B_2O_3 at 806 cm^{-1} is assigned to the vibration of diborate groups $(B_4O_7)^{2-}$, which is the typical glass network structure with non-bridging oxygen formed by added lithium ion [22]. It is estimated from Raman spectra of B20P30 that the amount of Li added into glass network is believed to reach its limit, ~50 mol% while in the B20P80 and B20P60 it is below 50 mol% due to increase of $POCl_3$.

Fig. 5 also shows that the peak at 780 cm^{-1}, shown in borate glass with lithium ion, decreased, the peak at 1110 cm^{-1}, the combination of various P—O groups with $(B—O—P)^{1-}$ and $(B—O—P)^0$, grew, and the peak at 715 cm^{-1}, P—O—P bridging bond, increased with increasing $POCl_3$ [23,24]. With increasing P_2O_5, the peak at the 1000 cm^{-1}, the overlapped peak of various phosphate group and the $(B—O—P)^0$ unit, eventually converted to 1110 cm^{-1} peak, the overlapped peak of various phosphate group and the $(B—O—P)^-$ unit. In overall, this result shows that the change from $(B—O—P)^0$ with $(P_4O_{13})^{6-}$ and $(P_3O_{10})^{5-}$ groups to $(B—O—P)^-$ with $(P_2O_4)^{4-}$ groups causes a shift of peak position and this suggests that the number of non-bridging oxygen increased significantly.

This observation is supported by the FT-IR measurement. Fig. 6 presents the variation of FT-IR spectra of B20P80 glass electrolyte compared to that of glass soot. The peak at 1375 cm^{-1} observed in glass soot was shifted to high frequency. The peaks at approximately 1000 cm^{-1}, P—O with non-bridging oxygen and the peak at 1180 cm^{-1}, the stretching band of BO_3 with a non-bridging oxygen, grew significantly. From this result it is inferred that the P=O formed in glass soot convert to the P—O with non-bridging oxygen and B—O bond also converted to the bond with non-bridging oxygen by heat treatment, which result in increased ion conductivity.

The variation of FT-IR spectra of glass electrolyte with various compositions are shown in Fig. 7. The sharp peak at 1200 cm^{-1} in B20P30 is the vibration of crystalline B_2O_3. With increasing $POCl_3$, this peak reduced and the peak at 1000 cm^{-1}, P—O with a non-bridging oxygen, increased significantly.

From results of the Raman spectra, FT-IR spectra, and conductivity, it is concluded that the conductivity was increased by significant increase of P—O and B—O bonds with non-bridging oxygens.

The exact reason of this significant increase of non-bridging oxygen is not clear at this stage. However, one of the reasons might be the homogenization of Li ion during the heat treatment. Some of Li in the form of an amorphous oxide will reacts with other oxide during the heat treatment and this homogenization will distribute the Li ions and incorporate into glass network, which will produce large number of non-bridging oxygens.

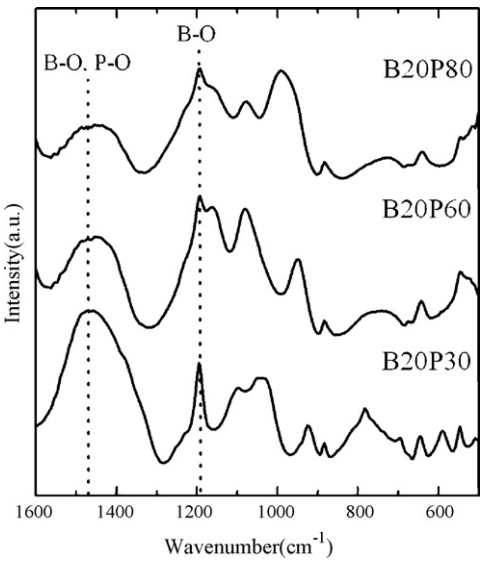

Fig. 7. FT-IR spectra of glass electrolyte fabricated from the deposited glass soot.

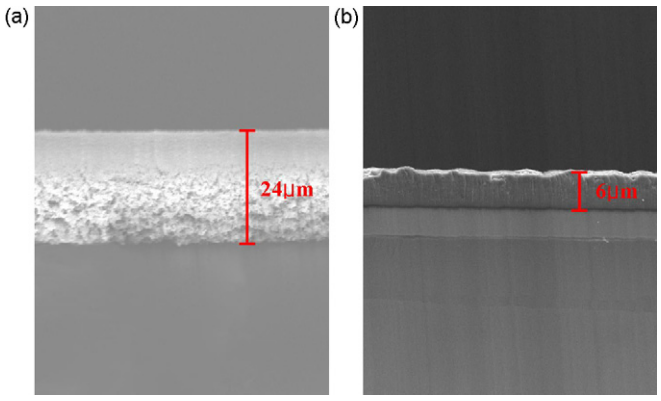

Fig. 8. Cross sectional images of deposited glass soot and sintered film. (a) Glass soot synthesized at flow rate BCl3: 20 sccm, $POCl_3$: 80 sccm and Li: 0.4 mol% on a silicon wafer before heat treatment, and (b) the dense thin film obtained by heating the deposited soot film at 600 °C for 2 h.

The exact reason of this significant increase of non-bridging oxygen is not clear at this stage. However, one of the reasons might be the homogenization of Li ion during the heat treatment. Some of Li in the form of an amorphous oxide will react with other oxide during the heat treatment and this homogenization will distribute the Li ions and incorporate into glass network, which will produce large number of non-bridging oxygens.

To fabricate the thin film electrolyte, the glass soot was deposited about 20 μm at condition of B20P80 as shown in Fig. 8(a). Fig. 8(b) shows the cross section of dense film after heat treatment at 600 °C. The deposition rate estimated after the consolidation was 0.3 μm min^{-1}.

4. Conclusions

The Li_2O–B_2O_3–P_2O_5 inorganic glass electrolytes were deposited by aerosol flame deposition at various flow rates of $POCl_3$. The conductivity increased with increasing P/(B + P) ratio and reached to 10^{-6} S cm^{-1} at room temperature. This conductivity is comparable to that of LiPON. Dense and uniform thin film electrolyte of 6 μm thick was fabricated on a Si wafer by aerosol flame deposition and subsequent heat treatment at 600 °C. The deposition rate estimated was 0.3 μm min^{-1}, which is much faster that the conventional vacuum deposition techniques.

The significantly enhanced conductivity was turned out to be related to much higher P_2O_5 content which cannot be obtained from the bulk glass process and the increased number of non-bridging oxygen within glass network. The exact mechanism of the significant increase of the number of non-bridging oxygen is not clear. Further study is needed to clarify this observation.

In this work, it was demonstrated that aerosol flame deposition is a promising candidate for the fabrication of thin film glass electrolyte. In our laboratory, the fabrication process of thin film Li ion battery using aerosol flame deposition is under developing. This process enables the fast deposition of oxide cathode and anode film in ambient atmosphere.

Acknowledgement

This work was supported by the Ministry of Information & Communications, Korea, under the Information Technology Research Center (ITRC) Support Program.

References

[1] A. Levasseur, B. Cales, J.M. Reau, P. Hagenmuller, Mater. Res. Bull. 13 (1978) 205–209.
[2] R.L. Mozzi, B.E. Warren, J. Appl. Cryst. 3 (1970) 251–257.
[3] S.W. Martin, C.A. Angell, J. Non-Cryst. Solids 83 (1986) 185–207.
[4] J.P. Malugani, G. Robert, Mater. Res. Bull. 14 (1979) 1075–1081.
[5] K.I. Cho, S.H. Lee, D.W. Shin, Y.K. Sun, Electrochim. Acta 52 (2006) 1576–1581.
[6] C.G. Chol, M.Y. Jeong, T.G. Choy, J. Mater. Sci. 34 (1999) 6035–6040.
[7] K.H. Cho, H.H. You, Y.S. Youn, J.S. Kim, D.W. Shin, Electrochim. Acta 52 (2006) 1571–1575.
[8] R.A. Nyquist, R.O. Kagel, Infrared Spectra of Inorganic Compounds, Academic Press, 1971, P54.
[9] G.J. Exarhos, W.M. Risen, Solid State Commun. 11 (1972) 755–758.
[10] G.J. Exarhos, W.M. Risen, Chem. Phys. Lett. 10 (1971) 484–486.
[11] B.N. Nelson, G.J. Exarhos, J. Chem. Phys. 71 (1979) 2739–2747.
[12] J.J. Hugens, S.W. Martin, J. Am. Ceram. Soc. 76 (1993) 1691–1696.
[13] M. Abid, A. Shaim, M. Et-tabirou, Mater. Res. Bull. 36 (2001) 2453–2461.
[14] M.J.G. Jak, E.M. Kelder, Z.A. Kaszkur, J. Pielaszek, J. Schoonman, Solid State Ionics 119 (1999) 159–164.
[15] M. Tatsumisago, H. Morimoto, H. Yamashita, T. Minami, Solid State Ionics 136-137 (2000) 483–488.
[16] E.M. Kelder, M.J.G. Jak, F. de Lange, J. Schoonman, Solid State Ionics 85 (1996) 285–291.
[17] D. Ravaine, J. Non-Cryst. Solids 38–39 (1980) 353–358.
[18] S.H. Lee, K.I. Cho, J.B. Choi, D.W. Shin, J. Powder Sources 162 (2006) 1341–1345.
[19] M. Irion, M. Couzi, A. Levasseur, J.M. Reau, J.C. Brethous, J. Solid State Chem. 31 (1980) 285–294.
[20] W.L. Konijnendijk, J.M. Stevels, J. Non-Cryst. Solids 18 (1975) 307–331.
[21] F.L. Galeener, G. Lucovsky, J.C. Mikkelsen, Phys. Rev. B 22 (1980) 3983–3990.
[22] J. Lorosch, M. Couzi, J. Pelous, R. Vacher, A. Levasseur, J. Non-Cryst. Solids 69 (1984) 1–25.
[23] D. Ilieva, B. Jivov, G. Bogachev, C. Petkov, I. Penkov, Y. Dimitriev, J. Non-Cryst. Solids 283 (2001) 195–202.
[24] J. Yifen, C. Xiangsheng, H. Xihuai, J. Non-Cryst. Solids 112 (1989) 147–150.